

# Design of portable electric and magnetic field generators

M G Stewart, W H Siew and L C Campbell†

Centre for Electrical Power Engineering, Department of Electronic and Electrical Engineering, Royal College, University of Strathclyde, 204 George Street, Glasgow, UK

E-mail: m.stewart@eee.strath.ac.uk, w.siew@eee.strath.ac.uk and l.campbell@clara.net

Received 28 June 2000, accepted for publication 29 August 2000

**Abstract.** Electric and magnetic field generators capable of producing high-amplitude output are not readily available. This presents difficulties for electromagnetic compatibility testing of new measurement systems where these systems are intended to operate in a particularly hostile electromagnetic environment. A portable electric and a portable magnetic field generator having high pulsed field output are described in this paper. The output of these generators were determined using an electromagnetic-compatible measurement system. These generators allow immunity testing in the laboratory of electronic systems to very high electrical fields, as well as for functional verification of the electronic systems on site. In the longer term, the basic design of the magnetic field generator may be developed as the generator to provide the damped sinusoid magnetic field specified in IEC 61000-4-10, which is adopted in BS EN 61000-4-10.

**Keywords:** electric field generator, magnetic field generator, IEC 61000-4-10, Tesla coil

## 1. Introduction

Electric and magnetic field generators that are capable of producing high-amplitude output fields are generally not readily available. This is perhaps historical in that most generators tended to be designed to facilitate testing to the different standards specified for electromagnetic compatibility in an environment equivalent to a far field of up to  $10 \text{ V m}^{-1}$ . In recent years, two new standards have been introduced to facilitate high-amplitude magnetic field testing. These are the damped oscillatory magnetic field immunity test (IEC 61000-4-10 [1], which requires field amplitude up to  $100 \text{ A m}^{-1}$ ) and the pulsed magnetic field immunity test (IEC 61000-4-9 [2], which requires field amplitude up to  $1000 \text{ A m}^{-1}$ ). At the time of writing this paper, the equipment to produce the fields specified was still not commercially available.

In this paper, we describe the design and construction of a high-amplitude electric field generator as well as a high-amplitude magnetic field generator. Both generators are portable and they were designed to be used either in or outside a laboratory environment. The radiated fields were measured using an in-house designed system and the system was reported in various conferences [3–5]. The generators described in this paper also form the basis for the design of generators to implement IEC 61000-4-10.

The portable generators were designed to fulfil two objectives. These were

- (1) to verify a measurement system's immunity to radiated interference in the laboratory before going on site and
- (2) to check the operation of a measurement system once set up on site. This is to verify that possible damage and/or malfunction arising as a result of transporting a system over long distances has not happened.

The specifications required to fulfil both objectives are similar. The *E*-field generator was designed to give a nominal output of  $250 \text{ kV m}^{-1}$ , with a ringing frequency of 600 kHz and the *H*-field generator was designed to give a nominal output of  $50 \text{ A m}^{-1}$ , with a range of frequencies between 20 and 50 MHz.

## 2. E-field generator

### 2.1. Theoretical design

Towards the end of the 19th century, many research laboratories were investigating the diverse effects associated with the new and evolving high voltage devices. One experimenter in particular, Nikola Tesla, developed a special high voltage transformer, designed around a coupled resonant circuit, which could be easily adapted and used in many HV AC experiments [6]. This type of transformer found favour with the leading experimenters working on AC systems, usually with frequencies in the tens of kilohertz or above.

Tesla coil circuits slowly began to lose favour as a source of high voltage in the 1940s, when Cockcroft–Walton circuits became available as a source for DC high voltage. These multiplier circuits, which involved multi-stage rectification,

† Retired. Cairntoul, 36 Hillside Terrace, Milton of Campsie, Kirkintilloch, Glasgow, UK.

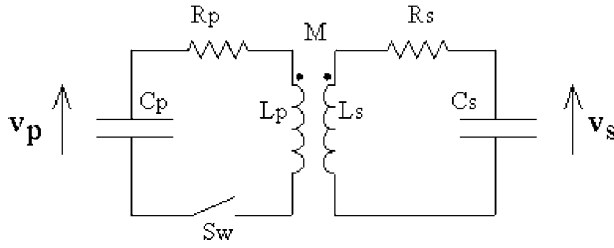


**Figure 1.** Loosely coupled transformer equivalent circuit.

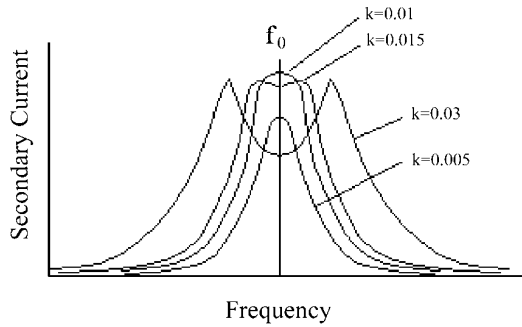


**Figure 2.** Frequency against secondary current in a loosely coupled circuit [7].

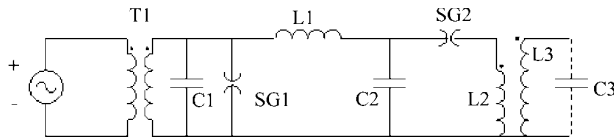


**Figure 3.**  $E$ -field generator circuit arrangement.

became practical with the development of the diode and as a result little further development took place on the Tesla coil.

Tesla coils, however, were not forgotten, and over the years have been put to various uses, e.g. as accelerating sources for fundamental physics experiments, as general purpose high voltage sources and also in the investigation of lightning effects. The concept also forms the basis of our  $E$ -field generator.

In the first circuit (figure 1) a loosely coupled air-cored transformer (Tesla coil) is used to provide resonant voltage gain at a particular frequency. In this arrangement, a capacitor  $C_p$  is charged by a high voltage source, and a switch  $Sw$  is used to close the circuit.  $R_p$  and  $L_p$  are the effective resistance and inductance respectively of the primary winding. This primary circuit is loosely coupled (by a mutual inductance  $M$ ) to a secondary circuit consisting of effective inductance ( $L_s$ ), effective resistance ( $R_s$ ) and effective capacitance ( $C_s$ ).

If the two circuits are resonant at the same frequency, the resulting behaviour is governed by the amount of coupling. If the coupling is small, the secondary current is small, and the plot of secondary current versus frequency has a shape as shown in figure 2 for a coupling coefficient,  $k$ , of 0.005. With an increase in coupling the secondary current increases, and the sharpness of the secondary current curve is reduced. As coupling is increased there comes a point (called critical coupling) where the secondary current is at its maximum value,  $k = 0.01$  in figure 2. With greater coupling still, the

secondary current curves starts to show a double hump, and the magnitude of the peaks reduces, the spread of frequencies increases and the humps start to move apart.

When the switch is closed, current passes around the primary  $LC$  circuit with a resonant frequency dependent on the values of  $L_p$  and  $C_p$  with a relationship defined as:

$$f_0(E) = \frac{1}{2\pi(L_p C_p)^{1/2}} \quad (1)$$

where  $f_0(E)$  is the resonant frequency of the  $E$ -field generator (Hz),  $L_p$  the primary inductance (H) and  $C_p$  the primary capacitance (F).

At this frequency the reactances of the inductor and capacitor are equal but opposite, and cancel out each other, giving a circuit which appears only as a low resistance, and hence allowing a high current to flow in the secondary.

The secondary voltage at resonance for the coupled circuit of figure 1, and in the particular case where both circuits are resonant at the same frequency is given by [7]:

$$v_s = v_p \left( \frac{L_s}{L_p} \right)^{1/2} \left( \frac{k}{k^2(Q_p Q_s)^{-1/2}} \right) \quad (2)$$

where  $v_s$  is the instantaneous secondary voltage (V),  $v_p$  the instantaneous primary voltage (V),  $L_s$  the secondary inductance (H),  $L_p$  the primary inductance (H),  $k$  the coefficient of coupling,  $Q_p$  the primary circuit quality factor and  $Q_s$  the secondary circuit quality factor, which is maximum for the condition where the coupling  $k$  is equal to the critical coupling  $k_c$ :

$$k_c = (Q_p Q_s)^{-1/2} \quad (3)$$

where

$$Q_p = \omega_0 L_p / R_p \quad (4)$$

$$Q_s = \omega_0 L_s / R_s \quad (5)$$

and

$$\omega_0 = 2\pi f_0 \quad (6)$$

where  $\omega_0$  is the resonant angular frequency ( $\text{rad s}^{-1}$ ).

The gain of typical Tesla coils is usually within the range 10 to 30.

## 2.2. Construction

The Tesla coil (figure 3) is powered by a 240 V/15 kV neon sign transformer T1 which is protected by a spark gap (SG<sub>1</sub>), and 150 pF capacitor ( $C_1$ ) on the HV side. The source voltage may be controlled by a variac. The output of the transformer is connected to a capacitance ( $C_2$ ) of 0.01  $\mu\text{F}$  via a 100 mH inductor ( $L_1$ ) which acts as further protection to the supply. The capacitor is connected first to the main spark gap (SG<sub>2</sub>) and then to a flat spiral inductor ( $L_2$ ), with inductance 5  $\mu\text{H}$ , made from 12 mm copper tube. Tubing is used instead of wire in order to keep the total circuit resistance low at high frequencies. The secondary circuit is made from an inductive coil ( $L_3$ ) made from 600 turns of small diameter PTFE insulated wire, which has a total length close to a quarter wavelength at the desired frequency, wound on a 100 mm diameter polythene former. The inductance

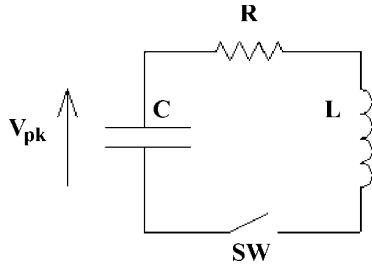


**Figure 4.** *H*-field generator equivalent circuit.

of this coil is 3 mH. At the top is connected an aluminium toroid of 0.75 m diameter, acting as top capacitance ( $C_3$ ). The bottom end of the secondary is connected to ground.

When the capacitor  $C_2$  is charged to a sufficient voltage, the main spark gap breaks down and current flows around the primary circuit. This induces a high voltage on to the secondary, which is at a maximum on the capacitive top plate. The frequency of the primary circuit may be tuned exactly to that of the secondary by altering the tapping point on inductor  $L_2$ . The circuit can be tuned to give critical coupling, and hence maximum voltage gain, by raising or lowering the position of the secondary within the primary coil thereby altering the coefficient of coupling.

### 3. *H*-field generator

#### 3.1. Theoretical design

A high-frequency *H*-field is produced by a large resonant peak current flowing around a low impedance circuit (figure 4).

A capacitor  $C$  is charged to a high voltage, and when switch  $Sw$  is closed, current flows around the circuit. The frequency of oscillation of the current is a function of the loop inductance  $L$  and capacitance  $C$ . Resistance  $R$  represents the resistance of the circuit leads etc.

The surge impedance of the circuit is

$$Z_0 = \left(\frac{L}{C}\right)^{1/2} \quad (7)$$

where  $Z_0$  is the surge impedance ( $\Omega$ ),  $L$  the inductance (H) and  $C$  the capacitance (F) and the peak current is given by

$$I_{pk} = V_{pk}/Z_0 \quad (8)$$

where  $I_{pk}$  is the peak current (A) and  $V_{pk}$  the peak capacitor voltage (V).

The resonant frequency of the *H*-field generator in Hz is

$$f_0(H) = \frac{1}{2\pi(LC)^{1/2}}. \quad (9)$$

#### 3.2. Construction

To produce a high *H*-field, a high circulating current is required. A nominal peak current of 100 A, with a variable frequency of between 20 and 50 MHz, was chosen. The circuit is as shown in figure 5. A 50 Hz charging source,

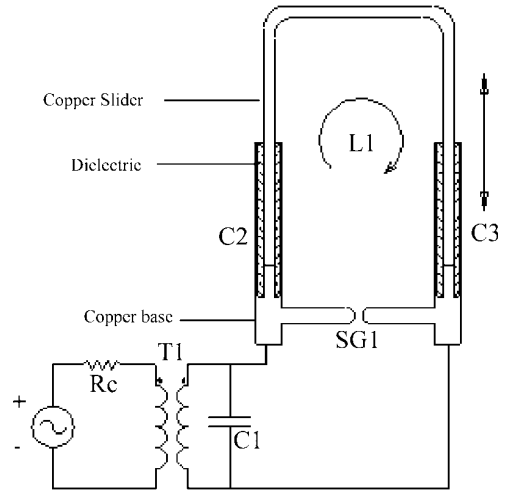


**Figure 5.** *H*-field generator circuit arrangement.

which is current limited by resistor  $R_c$ , feeds a step-up voltage transformer  $T_1$ . The output of the transformer charges capacitor  $C_1$  and the  $C_2/C_3$  network. The inductance  $L_1$  is the variable self-inductance of the loop. At the high frequencies being considered, the values of  $C_2$  and  $C_3$  are in the range of tens of picofarads and  $L_1$  of the order of microhenries. The function of  $C_1$  is to supply the energy to break down the spark gap  $SG$  and allow the lower energy stored in the  $C_2/C_3$ ,  $L_1$  circuit to oscillate at the desired frequency. The capacitors  $C_2$  and  $C_3$  have been constructed coaxially from copper tubes with a polypropylene dielectric separating them.

Increasing or decreasing the capacitance can be achieved by changing the position of the central conductor with relation to the outer. Since this also changes the circuit inductance, the circuit has a degree of tunability.

### 4. *E*- and *H*-field measurement systems

The two sensors used in the field measurement system are transient electromagnetic field sensors, which are based on a generic design. The complete measurement system used is described in detail in [3–5]. As a summary, the sensors are passive devices based on the asymptotic conical dipole design (*E*-field) and the multi-gap loop design (*H*-field). The outputs of the two sensors are the following.

*E*-field:

$$v_0 = A_{eq} R \epsilon_0 \frac{dE}{dt} \quad (10)$$

where  $v_0$  is the instantaneous output voltage (V),  $A_{eq}$  the sensor effective area ( $0.981 \times 10^{-2} \text{ m}^2$ ),  $R$  the sensor resistance ( $50 \Omega$ ),  $\epsilon_0$  the permittivity of free space ( $8.854 \times 10^{-12} \text{ F m}^{-1}$ ) and  $E$  the instantaneous electric field ( $\text{V m}^{-1}$ ).

*H*-field:

$$v_0 = A_{eq} \mu_0 \frac{dH}{dt} \quad (11)$$

where  $v_0$  is the instantaneous output voltage (V),  $A_{eq}$  the sensor effective area ( $0.908 \times 10^{-3} \text{ m}^2$ ),  $\mu_0$  the permeability of free space ( $4\pi \times 10^{-6}$ ) and  $H$  the instantaneous magnetic field ( $\text{A m}^{-1}$ ). From equations (10) and (11), it can be seen that the output voltage is dependent upon both the field amplitude and the frequency of the transient.

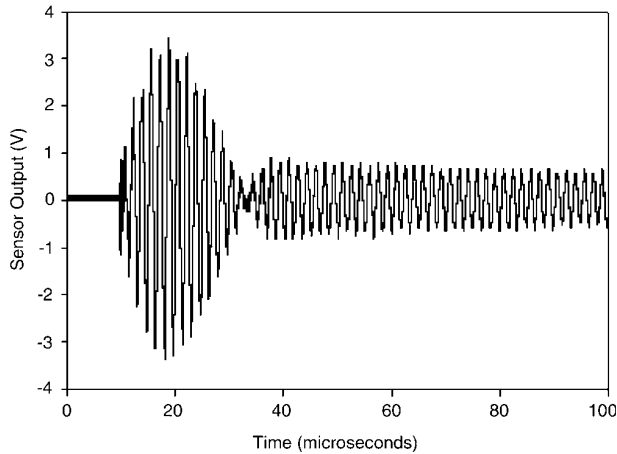


**Figure 6.** *E*-field sensor output against time.

The frequency response of both sensors is guaranteed to range from a lower 3 dB point of 250 kHz to an upper 3 dB point of 250 MHz. In practice, the calibrated response does not drop to 3 dB until 150 kHz and extends to 500 MHz before dropping below 3 dB.

Optical fibre was chosen as the transmission medium of the signal from sensors to the data acquisition equipment. This provides complete electrical isolation between the equipment out in the substation (when the measurement system is used in a substation) and that at the data acquisition site, thus removing the risk of corruption of the signal being transmitted.

The optical transmitter consists of a signal conditioner and an LED source. The signal conditioner is primarily to provide an interface to match the output of the sensors to the input characteristics of the LED. Since the sensors are completely passive they cannot be relied upon to provide any power with which to drive the LED. Therefore the signal conditioner takes the voltage developed at the sensor output and converts it to a current suitable to drive the LED. In addition, the signal conditioner can also provide any gain or attenuation that may be required.

The signal is transmitted over 100 m of fibre to the receiving equipment. The optical receiver consists of a PIN photodiode and further signal conditioning. The signal conditioning at this end is effectively a high gain current-to-voltage converter, which takes the small current developed by the PIN photodiode and transforms it into a 0–5 V signal. This can be input to one of two, four-channel, 2 Gsamples s<sup>-1</sup>, 1 MB per channel digitizing oscilloscopes (DSO).

The information, having been captured and digitized in the oscilloscope, could then be downloaded to a portable PC over a GPIB (general purpose interface bus) for storage. Processing of the stored data, such as fast Fourier transforms, to determine the field strength as a function of frequency, could then be performed.

### 5. *E*-field generator output

The sensor was placed 1 m from the Tesla coil, positioned parallel to the lines of electric field, and connected to the DSO. Figure 6 shows a typical trace record from the DSO,

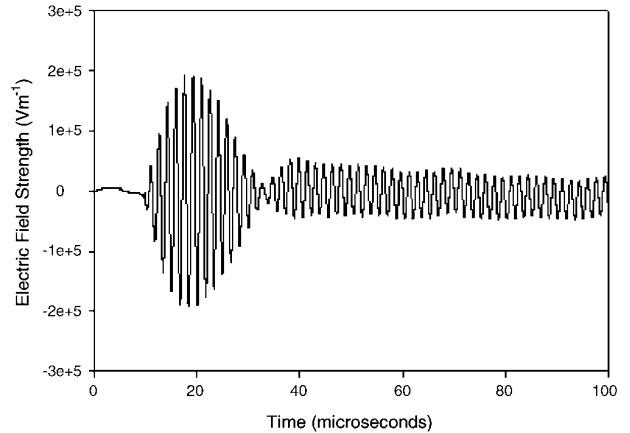


**Figure 7.** Electric field strength against time.

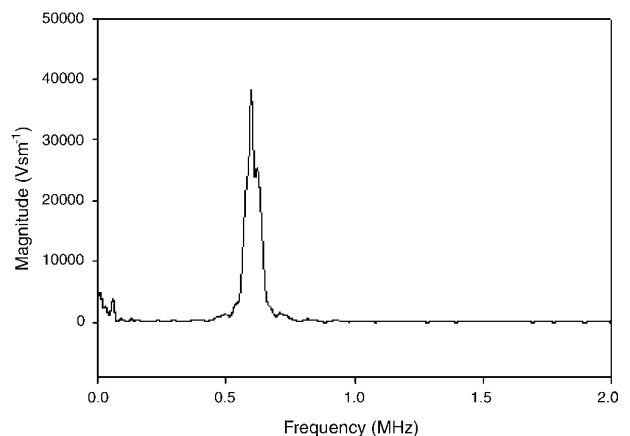


**Figure 8.** Electric field spectrum.

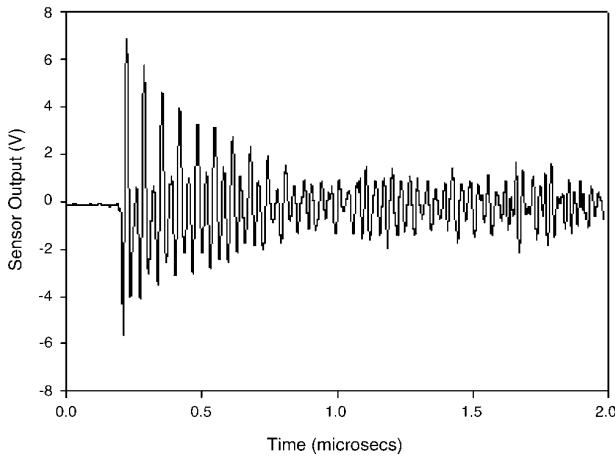
and figure 7 shows the integrated and factored result (using equation (10)) of the same trace and is thus shown as a plot of electric field ( $V m^{-1}$ ) against time.

Figure 8 shows the frequency-resolved spectrum of the field, which is centred on 600 kHz.

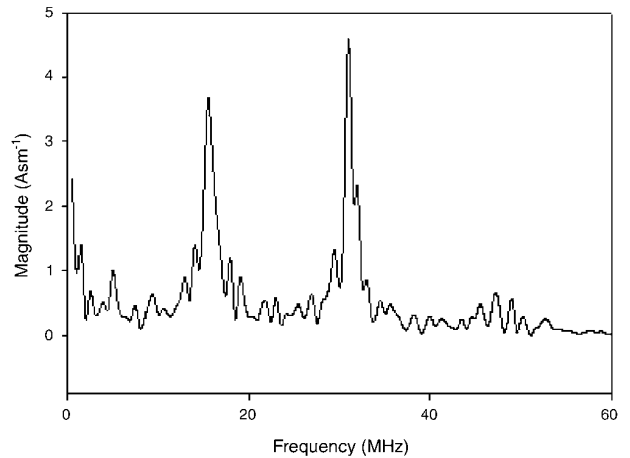
### 6. *H*-field generator output

Figure 9 shows an example of the signal recorded by the magnetic field sensor as captured by a digital sampling oscilloscope (in this case with the slider at position 4 corresponding to a designed frequency of 31 MHz). The voltage applied across the gap was 5 kV p-p and the sensor was placed inside the loop of the field generator. The signal was then integrated and multiplied by the appropriate factors (using equation (11)) and the result is as shown in figure 10, with the y-axis now in amps per metre. Figure 11 shows the frequency spectrum of the magnetic field, showing two peaks, one at the designed frequency (31 MHz) and the other at 15 MHz. With reference to figure 5, the 15 MHz peak is caused by  $C_1$  discharging into  $SG_1$  through the circuit lead inductance.

The field output for a range of different positions of the slider has been computed, position 1 being with the slider at its maximum extension, and position 6 at its lowest position.



**Figure 9.** *H*-field sensor output against time.



**Figure 11.** Magnetic field spectrum.

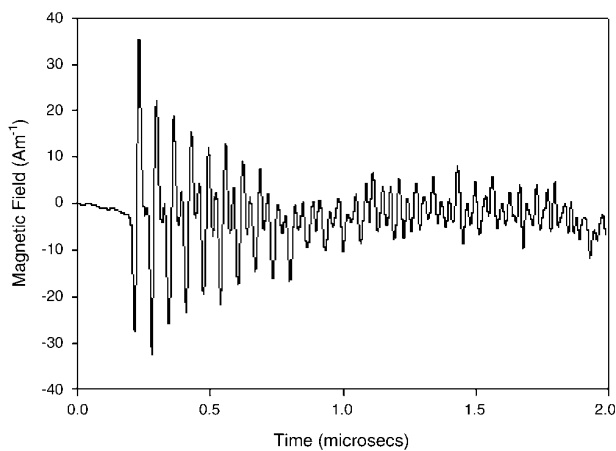


**Figure 10.** Magnetic field strength against time.

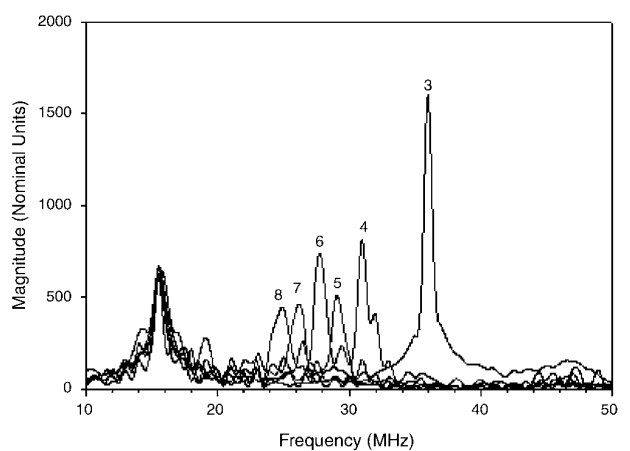


**Figure 12.** Normalized spectrum data showing variation with slider position.

The difference in height between each of the positions is 50 mm.

The frequency spectrum was normalized using the 15 MHz signal as a base, and these normalized spectra are labelled 3 to 8 in figure 12.

## 7. Use of the generators

The field generators were set up in the laboratory to check the immunity of both the radiated and conducted interference measuring systems during their development. Since the systems were to be used in the electrically noisy environment of an electrical substation during primary plant switching, it was important that the systems would not be affected by spurious signal pick-up.

The portability of the field measurement system allowed the operation of the field measurement system to be checked after the systems were set up on site.

Immunity of the field measurement systems was confirmed by blanking off the input to a sensor input to the optical transmitter and recording the output from the corresponding receiver on the oscilloscope. This was done for each of the channels.

In the case of the conducted measurement system the voltage probes were shorted and connected to earth, and

a shorting wire was used through the current sensor. The sensors were connected to the optical links and the outputs connected to the oscilloscopes. Again, the outputs could be checked for immunity.

## 8. Conclusions

The generators described have been used to check the immunity to transients of a fairly complex radiated field and conducted interference measurement system, throughout its development and use. The operation of field measurement systems and the integrity of ancillary electronic systems in areas of high field have been tested, and areas of concern were quickly identified and rectified.

The portability of the equipment also allowed for checking of the measurement systems in the field prior to the commencement of measurements and increased the confidence of operation in a measurement programme which required costly outages to set up the measurement system.

Generators such as these are low cost and simple to operate and can be useful where budgets do not allow the use of more specialized equipment.

The *H*-field generator may be a basis for the design of the equipment required for implementing IEC 61000-4-10.

## References

- [1] BS EN 61000-4-10 1994 EMC part 4: testing and measurement techniques, section 10: damped oscillatory magnetic field immunity test (London: British Standards Institute)
- [2] BS EN 61000-4-9 1993 EMC part 4: testing and measurement techniques, section 9: pulse magnetic field immunity tests (London: British Standards Institute)
- [3] Barrack C S, Siew W H and Pryor B M 1996 Review of the methods available for the measurement of transient electromagnetic interference in substations *Int. Conf. on Large High Voltage Systems, CIGRE 1996, (Paris, 1996)* paper 36-202
- [4] Barrack C S, Siew W H and Pryor B M 1997 The measurement of fast transient electromagnetic interference within power system substations *IEE 6th Int. Conf. on Developments in Power System Protection (Nottingham, 1997) IEE Conf. Publication 434*, pp 270–3
- [5] Barrack C S, Stewart M G, Shen B L, Siew W H, Campbell L C, Chalmers I D, Pryor B M, Muir F C and Walker K F 1999 Fast transient radiated and conducted electromagnetic interference measurement within power system substations *11th Int. Symp. on High Voltage Engineering (1999) IEE Conf. Publication 467*, vol 1, pp 1.343.P6–1.346.P6
- [6] Campbell L C and Stewart M G 1998 *E* and *H* field generators for pulsed interference testing in EHV systems *Pulsed Power 98, IEE Symp. (London, 1998)* paper 43
- [7] Termann F E 1943 *Radio Engineers' Handbook* (New York: McGraw-Hill) p 154